Internal dielectronic excitation in highly charged ions colliding with surfaces

G. A. Machicoane,[1,2] T. Schenkel,[1] T. R. Niedermayr,[1,2] M. W. Newmann,[1,3] A. V. Hamza,[1] A. V. Barnes,[1] J. W. McDonald,[1] J. A. Tanis,[4] and D. H. Schneider[1]

[1]*Physics & Space Technology Directorate, Lawrence Livermore National Laboratory, University of California, Livermore, California 94550*

[2]*Equipe de Recherche Ion-Surface, Université Pierre et Marie Curie, Paris 75005, France*

[3]*Department of Physics, University of Connecticut, Storrs, Connecticut 06269*

[4]*Department of Physics, Western Michigan University, Kalamazoo, Michigan 49008*

(Received 18 June 2001; published 2 April 2002)

Internal dielectronic excitation (IDE) is a correlated atomic physics process that takes place when the deexcitation of a Rydberg electron is accompanied by the excitation of a more tightly bound electron, resulting in a doubly excited inner-shell configuration. Subsequent x-ray emission involving an electron transition to a shell that initially contained no vacancies identifies the IDE process. IDE is mediated by the electron-electron interaction in a manner similar to a time-reversed Auger transition, and can occur during the neutralization of a slow highly charged ion interacting with a solid where there are many Rydberg levels that can give rise to correlated transitions to degenerate energy states. We have investigated IDE for a wide range of projectiles and solid targets by measuring the resulting x-ray emission. The characteristic features of the x-ray spectra suggest that IDE occurs above the surface of the solid.

DOI: 10.1103/PhysRevA.65.042903 PACS number(s): 79.20.Rf

I. INTRODUCTION

The interaction of slow highly charged ions with surfaces has been an emerging field in atomic collision physics during the past decade [1,2]. Because of the large amount of potential energy that very highly charged ions carry with respect to their kinetic energy, the interaction of such ions with a surface is characterized by features such as hollow atom formation, large electron emission, and material ablation [1,2]. These features are relevant for applications in nanotechnology such as surface analysis and surface modification.

To date, much of the work involving the interaction of highly charged ions with surfaces has dealt mainly with low Z projectiles [2]. The dominant theoretical picture for the different processes occurring during these interactions has been given within the framework of the classical-overbarrier model (COB) of Burgdörfer and co-workers [3]. In this picture, an ion with its inner shell empty approaching a surface captures electrons resonantly into high-lying Rydberg states at a critical distance from the solid leading to hollow atom formation. Due to the very short but finite time (fs) that the ion spends above the surface, the ion is still in a highly excited state when it enters the solid. The inverse of the plasmon frequency of the near-surface region is a characteristic time, within which a more compact hollow atom is formed below the surface.

The fact that the inner shell (mostly K and L) of the ion survives the close collision has already been demonstrated with low-Z ions in experiments involving KLL Auger measurements [2]. In the case of Ar^{17+} ions striking a surface, the resulting x-ray spectrum showed that the filling of the initial K vacancy is due to decay below the surface [4]. In this particular case, capture takes place mainly into the M shell and subsequent decays lead to the filling of the L and the K shells. The main features of the observed Auger or x-ray spectrum were explained using a stepwise decay model for the hollow atoms. Since the energy of the emitted electron or photon depends on the number and shell location of the spectator electrons present at the time of decay, this energy can be used to determine the time of the decay.

For higher Z, highly charged ions, most of the inner shells are filled below the surface, and consequently, most of the potential energy is transferred to the degrees of freedom of the solid surface. Electron, ion, neutral particle, and x-ray emission account for only $\sim$10% of the potential energy of the slow, highly charged ion released upon collision with a surface [1]. Since the radiative rates for inner-shell vacancies increase as Z^4, the detection of x rays is the method suited to study this last stage of the neutralization process. Recently, the charge neutralization time of Th^{75+} incident on an amorphous carbon foil has been estimated to be around 7 fs [5]. The understanding of the fast decay times of inner shells is an active field of research [6,7] since it allows insight into the way that the initial potential energy of the ion is primarily deposited.

Recently, a new decay process for hollow atoms that takes place below or at the surface of a solid was identified. The process is referred to as internal dielectronic excitation (IDE) [8], and its existence was inferred from the observation of M x rays emitted from ions not containing initial M vacancies prior to interaction with the surface. The IDE process can come about, for example, if a $3lnl'$ $(n>4)$ state is energetically degenerate with a $4l4l'$ state. In this case, a transition can occur that resonantly excites an electron from the M shell into the N shell, creating an M vacancy, while another electron from a high n state simultaneously fills a vacancy in the N shell. This resonant transition is mediated by the electron-electron interaction in a manner analogous to a time-reversed Auger transition. The vacancy in the M shell can then subsequently decay radiatively and the resulting x ray can be observed. Thus, IDE is very similar to dielectronic recombination (DR), in which an initially free electron resonantly excites a bound electron and is itself simultaneously captured. Subsequent x-ray emission completes the DR process

resulting in recombination of the ion. The possibility for the occurrence of IDE is closely linked to the existence of a hollow atom that has some of its inner shells (in this case the *N* shell) transiently empty and, at the same time, possesses a large number of electrons in higher-lying shells. Deexcitation of this highly excited system causes electrons to quickly cascade through the empty shells as the system relaxes. The large number of possible transitions and the large number of energy configurations involved in the various decay processes make the necessary energy degeneracy quite probable [9].

The first experimental evidence for IDE was reported for uranium projectiles incident on a Be surface [8]. Calculations based on a Dirac-Hartree-Slater model showed $3lnl'$ states could in fact be degenerate with a $4l4l'$ state for $n \geqslant 8$. Furthermore, the calculations indicated that the probability for IDE to occur in uranium was about 80%. Here we report new measurements of IDE for a wide variety of projectiles ($Z = 54-90$) impinging on different surfaces ranging from metal to insulator. For ions with an initial vacancy in the *M* shell, a broad peak due to *M* x-ray emission was observed as expected. For ions with no initial *M* vacancy, a peak corresponding to *M* x rays was still observed meaning that an *M* vacancy was created in the interaction of the ion with the surface. Significant differences in the features of the measured *M* x-ray spectra were observed for the various projectiles used, but these features were essentially independent of the target.

II. EXPERIMENTAL PROCEDURE

Ions were extracted from the electron beam ion trap (EBIT) at the Lawrence Livermore National Laboratory. Ions were most often extracted at 7 keV, giving the ions a kinetic energy of $7\,\mathrm{keV} \times q$. A few measurements were also performed at 6, 5, and $3\,\mathrm{keV} \times q$ for thorium ions. No differences in the x-ray spectra were observed due to changing the kinetic energy of the ion in this kinetic-energy range. After charge-state selection, the ions were directed onto targets that consisted of ~100 nm foils (±10%) of diameter 2.54 cm. Five different foils were used in this work: Au, Ag, amorphous carbon, Si, and SiO_2. The pressure was less than 2×10^{-8} Torr. X rays were collected in transmission mode with an IGLET-X windowless germanium detector placed behind the foils. The detector had a resolution of ~150 eV full width at half maximum (FWHM) at 5.9 keV. The distance from the detector to the foils was 21 mm and the active diameter of the detector was 6 mm, giving a solid angle of ~0.06 sr. X rays were recorded over the energy range ~300–5000 eV for which the detector has an absolute efficiency close to 100%. Corrections were made to the measured x-ray yields for self-absorption in the foils.

A sputter gun placed at 90° with respect to the beam line was used to clean the foils using a Xe^+ beam that was directed onto the foils by means of an electrostatic bender. Sputter cleaning cycles of 15 min with a 1 μA beam were performed. Cleanliness of the foils was spot-checked by secondary ion mass spectrometry. The same bender was used to measure the ion current while the x-ray spectra were collected. The ion current was further calibrated against a Faraday cup biased to −300 V that could be placed at the same position as the foils. The energy calibration of the x-ray detector was performed using a radioactive ^{55}Fe source placed into the vacuum system for the high-energy part of the measured x-ray range, while x-ray emission from N^{6+} and O^{7+} ions was used for the low-energy part. The *K* x-ray energies of these ions are known [10] and have energies very close to those of the respective neutral atoms.

Sources of error in the absolute measurement of x-ray yields are the detection of x rays, the determination of the solid angle, and the determination of the integrated ion flux. At least 10 000 counts per spectrum were collected (except for the Xe^{26+} and below); taking the error as the square root of the number of counts gives an uncertainty of less than 1%. The error in the solid angle determination rests in the determination of the distance of the foils from the detector, which was determined to within 0.5 cm, yielding an error of 2.5%. The determination of the integrated ion flux was to within 0.5% of the 5% of the flux that was monitored. This yields a 2.6% error in the ion flux determination. The total estimated error is 6.1%. For the ratio of two measurements the solid angle error is removed, giving a total estimated error of 7.2%.

III. RESULTS

In Fig. 1, we show x-ray spectra resulting from the radiative deexcitation of incident Ni-like (no *M* vacancies) and Co-like (one *M* vacancy) xenon ($Z=54$), holmium ($Z=67$), gold ($Z=79$), and thorium ($Z=90$) ions interacting with the germanium detector surface for xenon, holmium, gold, and thorium and a silicon foil target for xenon. For each projectile species, the x-ray yield from ions having initially one vacancy in the *M* shell (Co-like core), i.e., Xe^{27+}, Ho^{40+}, Au^{52+}, and Th^{63+}, respectively, is greater than the yield from ions having initially no *M*-shell vacancies (Ni-like core), i.e., Xe^{26+}, Ho^{39+}, Au^{51+}, and Th^{62+}, respectively. However, as in the work of Ref. [8], it is significant that *M* x rays are observed for ions having no initial *M* vacancy. Thus, these results point to the existence of the IDE mechanism to create *M* vacancies in the interaction of the ion with the solid target.

In the spectra of Fig. 1, three features are notable: the shapes, the energy shifts, and the relative intensities of the *M* x-ray peak from ions with no initial *M*-shell vacancy compared to those with an initial *M*-shell vacancy. First, the width of the main peak for the Ni-like core is two to three times smaller than that for the Co-like core (except in the case of xenon). These *M* x rays consist mainly of $N \rightarrow M$ transitions. The main peak is due largely to unresolved $4f \rightarrow 3d$ transitions ($4p \rightarrow 3d$ transitions are also possible but are less likely to occur and constitute a shoulder on the low-energy side of the main peak) resulting from the multitude of electronic configurations that arise depending on the number of electrons captured and their distributions at the time of x-ray emission. Consequently, the narrower *M* x-ray peak for hollow ions (atoms) with no initial *M*-shell vacancy indicates

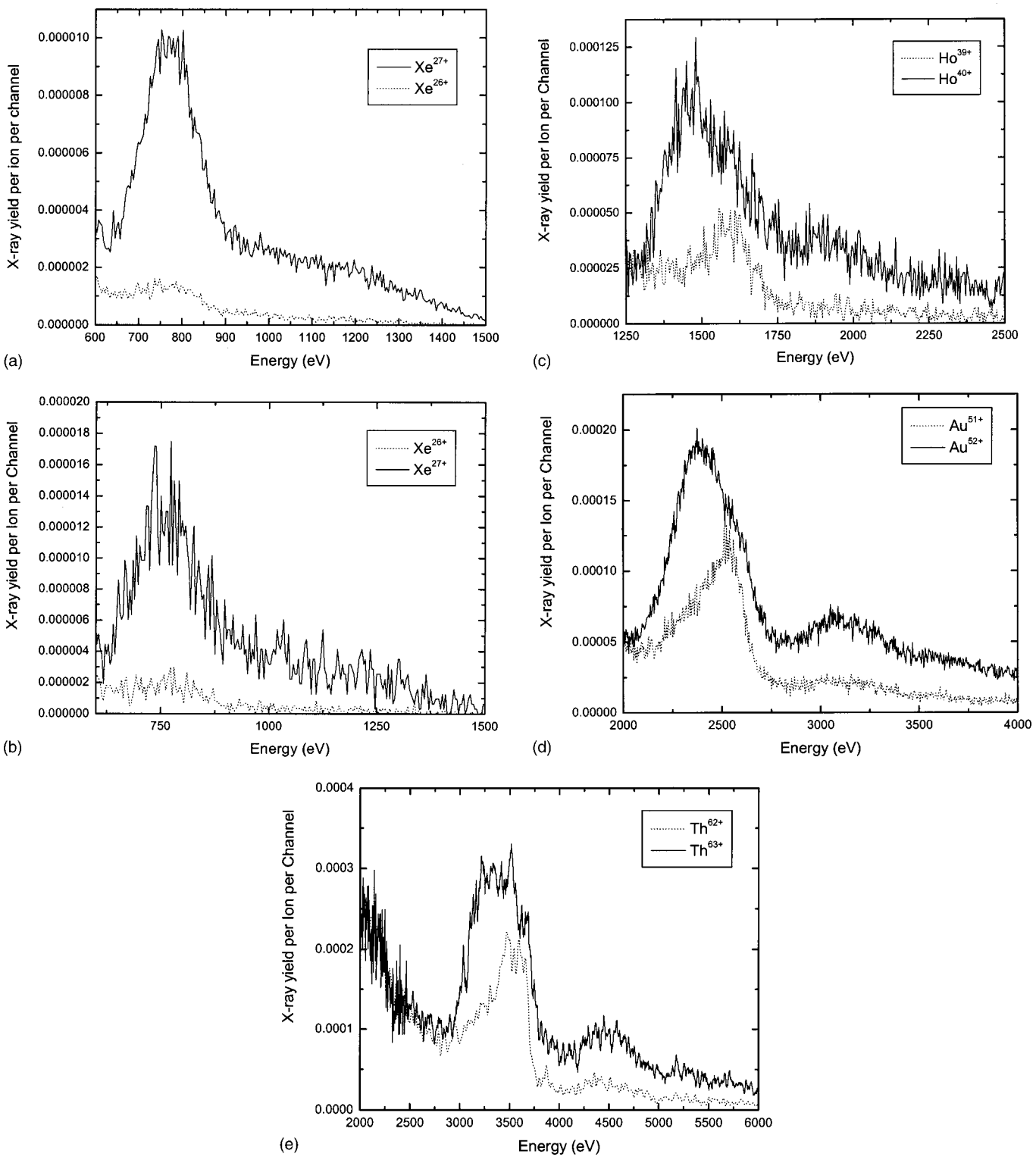

FIG. 1. Measured *M* x-ray spectra for incident xenon (a,b), holmium (c), gold (d), and thorium (e) projectiles having one (upper spectrum) or zero (lower spectrum) initial *M* vacancies, respectively. The xenon spectra in (b) were taken from collisions with a silicon foil, and the xenon in (a), holmium, gold, and thorium spectra were collected from collisions with a Ge target (i.e., the detector surface).

that x-ray emission takes place in the presence of fewer electronic configurations.

A shift in the energy of the main *M* x-ray peak for the Ni-like ions relative to the Co-like ions is also observed, with the magnitude of the shift increasing as the *Z* of the projectile increases. For thorium, this shift reaches ~250 eV whereas almost no shift is visible in the case of the xenon projectile. This shift to higher energies indicates either that the average number of ''spectator'' electrons at the time of the decay for the Ni-like ions is smaller than for the Co-like ions, or that

the spectator electrons exist in higher shells at the time of x-ray emission for incident Ni-like ions. In the latter case, this would mean that the transition takes place at an earlier stage of the neutralization process of the highly charged ion.

The third point concerns the relative intensities of the lines corresponding to zero or one initial M vacancy, respectively. It is seen that the peaks for ions with no initial M vacancy have a low-energy tail and that the intensities of these peaks are considerably smaller than those for ions with an initial M vacancy. Thus, the observed M x-ray yield is strongly dependent on whether or not the incident ion has an initial M vacancy as expected. Furthermore, for ions that initially have an M vacancy, the filling of this vacancy can occur through an electron transition from a higher shell $(O,P,\ldots)$, giving rise to x rays of higher energy. The high-energy tails of the spectra shown in Fig. 1 for ions with an initial M vacancy are found to extend to the binding energy of the $3d$ subshell. In the case of ions with no initial M vacancy, the intensity of these high-energy contributions is greatly reduced indicating a weak contribution from the higher shells.

IV. DISCUSSION

The IDE mechanism proposed in Ref. [8] can account for the features observed in the x-ray spectra of Fig. 1. Specifically, to create an M-shell vacancy in an ion not initially containing one and, subsequently, give rise to M x-ray emission, a $3d$ electron can be promoted to one of the $n=4$ subshells, while an electron in the one of the outermost shells is demoted to an $n=4$ subshell. For M x-ray emission to occur, either the promoted or the demoted electron must go to the $4p$ or $4f$ level. As mentioned above, this two-electron transition is attributed to the electron-electron interaction in a manner analogous to a time-reversed Auger transition.

Metastable states of the incoming ions as a source of M x rays can be ruled out. First, the distance from the trap to the target foil (4 m) and the low velocity ($<0.4v_{\mathrm{Bohr}}$) of the extracted ions requires a lifetime longer than 10^{-6} s for any metastable ion striking the target. Any nonradiative (autoionizing) decay has already occurred in the trap [11] and radiative decay would occur before the ion reached the target [12]. Second, the yield of M x rays decreases smoothly for ions with increasing N-shell occupation for thorium and holmium. The probability for metastable ions would be expected to decay more dramatically. Third, no L x rays were observed for Xe^{44+}, for which the ''stable'' ion has no L vacancies. Metastable ions were also ruled out as a source of M x rays in the IDE study by Schuch *et al.* [8].

In Fig. 2, we plot the x-ray yields obtained in the case of thorium projectiles impinging on the various surfaces studied. The x axis represents the incident thorium ion charge states involved in the interaction but expressed in terms of the number of vacancies in the M shell. Negative values refer to the number of electrons present initially in the N shell. It can be seen that the x-ray yield decreases smoothly as the number of electrons in the N shell increases for all the targets used. This shows the role played by N vacancies in the IDE mechanism as discussed above [8]. More important, however, is the observation that the M x-ray yield is nearly independent of the target used for ions with no initial M vacancies. This latter result rules out molecular orbital promotion as a mechanism for producing M vacancies since the probability for such promotion would be expected to vary strongly for the wide range of Z (atomic number) for the targets used. Moreover, the weak dependence of the x-ray yield on the target used points to an internal effect consistent with the IDE mechanism. As noted above, the x-ray emission for ions with no initial M-shell vacancies occurs at higher energy due to emission before filling of the N shell, i.e., few spectator electrons. Thus, the IDE mechanism occurs during the early stages of the ion neutralization process. The early stages of the neutralization (above surface capture) are controlled by the work function of the surface. The work functions for the targets used in this study are all approximately 5 eV. The lack of dependence of the IDE x-ray yield on the surfaces investigated is consistent with IDE occurring early in the neutralization.

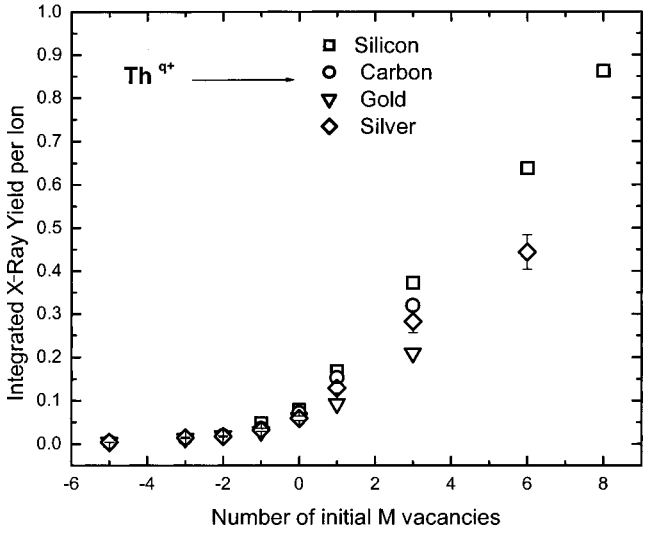

FIG. 2. Measured integrated M x-ray yields for thorium projectiles interacting with various targets. The x axis refers to the initial charge state of the ion expressed in terms of the number of initial vacancies in the M shell (Th^{63+} corresponds to one M vacancy). Negative values refer to the number of electrons initially present in the N shell. A very weak dependence of the x-ray yield on the target used is observed for the negative values (no M vacancies), whereas there is a stronger dependence of the yield on the target used for ions that carry initial M vacancies. A representative error bar is shown. See text for discussion of errors.

On the other hand, for thorium ions with an initial vacancy in the M shell, the measured x-ray yield exhibits a dependence on the target Z, with the highest yield occurring for the silicon target and the lowest yield for the gold target (Fig. 2). This result can be explained by considering the differences in the neutralization of highly charged ions striking insulators compared to metals. In the former case, the lower number of electrons available from the solid tends to increase the fluorescence yield due to slower filling of the inner shells, thereby reducing the competitive Auger deexcitation channel [13]. This conclusion is further supported by the observation (not shown) of a shift to higher x-ray energies

for the main *M* x-ray peak in the case of silicon compared to gold, a result which implies fewer *N*-shell electrons at the time of x-ray emission for silicon. Similar differences have been observed for all the projectiles with initial *M* vacancies used in this experiment. No such energy shift is observed, however, from one target to another for the *M* x-ray lines attributed to IDE (projectiles with no *M* vacancies).

At 2×10^{-8} Torr, the foil surfaces will remain clean for ~100 s from background gases that have a sticking probability of 1. The background gas consisted principally of hydrogen, water, and carbon monoxide. For clean gold and silver foils at room temperature, the residence time for water on the surface is nearly zero [14]. Molecular adsorption of hydrogen at room temperature is again near zero for all surfaces investigated. Dissociative adsorption of hydrogen is activated on all surfaces studied [15,16], yielding near zero coverage of atomic hydrogen. Carbon monoxide and water also have near zero residence time on the carbon foil surface at room temperature [17]. Carbon monoxide adsorption on silver and gold occurs readily only on partially oxidized surfaces. Gold and silver surfaces are difficult to oxidize at 10^{-8} Torr [13]. Carbon monoxide does not appreciably adsorb on silicon surfaces at room temperature [18]. While water has a fairly high sticking probability (~0.2) on silicon at low temperatures, at room temperature the sticking probability is low due to the short residence time of water in the mobile precursor state [19]. Thus, the foils used in this study—silicon, carbon, silver and gold—are particularly forgiving and will remain clean during the course of a measurement (~1000 s). The observation of no effect of the x-ray emission for Th^{q+} $58<q<62$ with a foil target is due to the IDE process occurring early in the neutralization process, and early neutralization is controlled by the work function of the surface. The work functions for these targets are all within 0.4 eV of 5 eV [20].

Finally, strong differences in the measured *M* x-ray yields for incident ions with no initial *M* vacancies are observed depending on the initial number of electrons in the *N* shell. These are the x rays that are attributed to the IDE mechanism. While only those ions with zero or one electron in the *N* shell give rise to *M* x rays for incident xenon and holmium, *M* x rays are observed for ions with up to six electrons in the *N* shell for gold and thorium.

Further analysis of the measured yields gives evidence that the IDE mechanism also exists for ions with an initial vacancy in the *M* shell. In the left part of Fig. 3, the x-ray yield for thorium projectiles divided by the initial number of vacancies in the *M* shell is plotted against the initial number of *M* vacancies. It is seen that this ratio tends to decrease with an increasing number of *M* vacancies. It would be expected, however, that this ratio should be constant if the *M* x-ray yield is nearly proportional to the number of initial *M* vacancies, or should increase slightly because of the reduced screening of the core for higher charge states, thereby resulting in a higher radiative rate. However, by subtracting the x-ray yield obtained for Ni-like ions (i.e., no *M* vacancy) from the total x-ray yield, and then dividing by the number of initial *M* vacancies, a more constant value of this ratio is obtained as seen in the right-hand side of Fig. 3, thus indicating an IDE contribution for ions with initial *M* vacancies. Evidence for this IDE contribution can also be seen directly from Fig. 1 for holmium, gold, and thorium projectiles, where there exists a structure on the high-energy side of the main peak for the upper spectrum corresponding to one initial *M* vacancy in each case. Furthermore, for Th^{63+} (one *M* vacancy) the radiative yield is nearly equal to the IDE yield for Th^{62+} in this high-energy region.

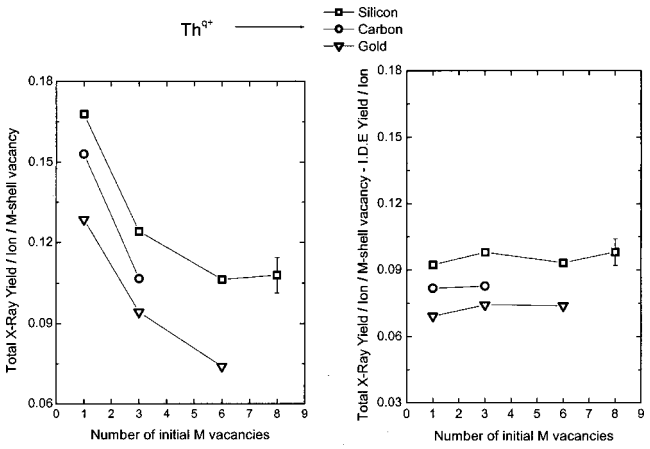

FIG. 3. *M* x-ray yields for thorium ions divided by the number of initial *M* vacancies. The targets used were silicon, carbon, and gold foils. Left: Total x-ray yields divided by the number of initial *M* vacancies. Right: Total x-ray yields minus the measured yield for incident ions without an *M* vacancy divided by the number of initial *M* vacancies. Representative error bars are shown in each panel. See text for discussion of errors.

From the measured data, it is possible to assess the importance of the IDE yield (for ions with no initial *M* vacancy) with respect to the ''normal'' radiative yield (for ions possessing an initial *M* vacancy) as a function of the *Z* of the projectile. In Fig. 4, we plot the ratio of the x-ray yield obtained from incident Ni-like ions to that obtained for inci-

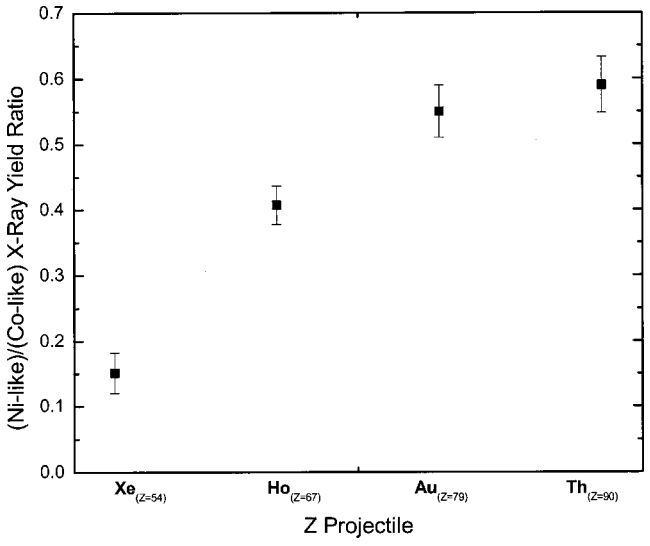

FIG. 4. Ratios of *M* x-ray yields for incident ions with no initial *M* vacancy to those for ions with one initial *M* vacancy as a function of the *Z* of the projectile for the data in Fig. 1.

dent Co-like ions. In the case of xenon, the ratio found is about 15%, whereas for thorium the ratio is nearly 60%. However, it is not clear if this strong projectile Z dependence reflects an increasing IDE probability with projectile Z because the fluorescence yield of the radiating ions must also be taken into account. In Ref. [8] it was assumed that the M-shell fluorescence yields for ions with and without initial M vacancies were equal. In this case, the IDE probability can be determined from the experimental measurement of the x-ray yields for ions with and without an initial M vacancy, respectively, if the value of fluorescence yield is known.

However, the M-shell fluorescence yields may not scale the same way for ions with or without an initial M vacancy. This is because there are apparently fewer N-shell electrons present at the time of x-ray emission in the case of the IDE as evidenced by the shift to higher energies for the x rays emitted by ions with no initial M vacancies. Additionally, strong differences in the fluorescence yield can arise from the differences in the dynamics of hollow atom formation and neutralization below the surface of the solid. As discussed above, based on their shapes, energy shifts, and relative intensities, M x rays resulting from IDE are likely to be emitted in an earlier stage of the hollow atom deexcitation process compared to M x rays emitted from ions with an initial M vacancy. Also, in going from xenon to thorium, the capture of electrons from the solid does not take place into the same shells. Capture takes place into those projectile shells closest in energy to the valence band of the solid [21]. This means that the principal quantum number n of the shell into which capture occurs increases with the Z of the projectile, thus leading to fewer N-shell electrons at the time of x-ray emission for higher Z values. In the case of xenon, for example, the shift in x-ray energy is very small for the IDE yield compared to the ''normal'' x-ray yield (see Fig. 1), but for xenon the N shell is very close to the continuum leading to very fast filling of this shell. In this case, the fluorescence yields associated with ions having zero or one initial M vacancy are likely to be nearly equal, thereby allowing a determination of the IDE probability from the x-ray yields directly (15% for xenon).

As the Z of the projectile increases, the filling of the N shell takes place more slowly and occurs mainly by cascading as evidenced by the observed increase in the yield of N x rays for higher Z (these results are not shown here). However, since the IDE mechanism is presumed to occur at an early stage of the hollow atom decay process, the electron demoted into the $4f$ subshell may then subsequently fill the vacancy created in the M shell by emitting an x ray. Thus, the IDE process enhances the probability for x-ray emission for the high-Z projectiles due to the lack of electrons present in the N shell, which effectively reduces the competitive Auger decay channel. Consequently, for holmium, gold, and thorium ions it is likely that the fluorescence yield associated with the decay of the vacancy created in the M shell in the IDE process is considerably larger than that associated with the decay of an M vacancy in the incident ion. For example, a fluorescence yield enhancement of a factor of 4 in the case of thorium projectiles with no M vacancies would give an IDE probability equal to that for xenon (see above).

V. CONCLUSION

In conclusion, M x-ray emission has been observed for a broad range of ions having no initial vacancy in the M shell following their interaction with various solid targets. Similar measurements were conducted for ions possessing initial M vacancies for comparison. The spectral features observed for the M x rays emitted from incident Ni-like ions, i.e., ions with no initial M vacancy, point to x-ray emission that takes place at an early stage of the hollow atom deexcitation process following the interaction of the highly charged ion with a surface. Here, early means before the electrons captured by the incident ion have time to cascade into the N shell. For incident ions without an initial M vacancy, the apparent independence of the observed M x-ray yield on the target used suggests a mechanism internal to the deexciting atomic system for producing the M vacancy. The features of the observed M x-ray spectra are consistent with the IDE mechanism proposed by Schuch *et al.* [8]. For incident ions having an initial M vacancy, the data indicate also an M x-ray contribution from IDE that competes with inner-shell filling below the surface in the neutralization process of highly charged ions. It remains unclear, however, whether the IDE probability increases with the Z of the projectile or if the observed increase in the M x-ray yield with increasing Z is related to more efficient radiative decay associated with differences in the dynamics of hollow atom neutralization from one ion to another.

ACKNOWLEDGMENTS

This work was performed under the auspices of the U.S. Department of Energy at the Lawrence Livermore National Laboratory under Contract No. W-7405-ENG-48 and also funded in part by the Chemical Sciences, Geosciences, and Biosciences Division, Office of Basic Energy Sciences. J.A.T. was supported in part by the Chemical Sciences, Geosciences, and Biosciences Division, Office of Basic Energy Sciences, U.S. Department of Energy.

[1] T. Schenkel, A. V. Hamza, A. V. Barnes, and D. H. Schneider, Prog. Surf. Sci. **61**, 23 (1999).

[2] A. Arnau, F. Aumayr, P. M. Echenique, M. Grether, W. Heiland, J. Limburg, R. Morgenstern, P. Roncin, S. Schippers, R. Schuch, N. Stolterfoht, P. Varga, T. J. M. Zouros, and HP. Winter, Surf. Sci. Rep. **27**, 113 (1997).

[3] J. Burgdörfer, P. Lerner, and F. W. Meyer, Phys. Rev. A **44**, 5674 (1991).

[4] J.-P. Briand, L. de Billy, and P. Charles, Phys. Rev. Lett. **65**, 159 (1990).

[5] M. Hattass, T. Schenkel, A. V. Hamza, and A. V. Barnes, Phys. Rev. Lett. **82**, 4795 (1999).

[6] S. Winecki, C. L. Cocke, D. Fry, and M. P. Stöckli, Phys. Rev. A **53**, 4228 (1996).
[7] R. Diez Muiño, A. Salin, N. Stolterfoht, A. Arnau, and P. M. Echenique, Phys. Rev. A **57**, 1126 (1998).
[8] R. Schuch, D. Schneider, D. A. Knapp, D. DeWitt, J. McDonald, M. H. Chen, M. W. Clark, and R. E. Marrs, Phys. Rev. Lett. **70**, 1073 (1993).
[9] A. Nuñez and N. Elander, Phys. Scr., **T73**, 311 (1997).
[10] J.-P. Briand, D. Schneider, S. Bardin, and H. Khemliche, Phys. Rev. A **55**, 3947 (1997).
[11] D. Schneider, D. DeWitt, M. W. Clark, R. Schuch, C. L. Cocke, R. Schmeider, K. J. Reed, M. H. Chen, R. E. Marrs, M. Levine, and R. Fortner, Phys. Rev. A **42**, 3889 (1990).
[12] Y. Yamazaki, Int. J. Mass. Spectrom. **192**, 437 (1999).
[13] G. A. Machicoane, T. Schenkel, T. R. Niedermayr, M. W. Newmann, A. V. Hamza, A. V. Barnes, J. W. McDonald, J. A. Tanis, and D. H. Schneider (unpublished).
[14] K. Bange, T. E. Madey, J. K. Sass, and E. M. Stuve, Surf. Sci. **183**, 334 (1987).
[15] A. G. Sault, R. J. Madix, and C. T. Campbell, Surf. Sci. **169**, 347 (1986).
[16] K. W. Kolasinski, Int. J. Mod. Phys. B **9**, 2753 (1995).
[17] R. B. Phelps, L. L. Kesmodel, and R. J. Kelley, Surf. Sci. **340**, 134 (1995).
[18] H. Ibach, K. Horn, R. Dom, and H. Lüth, Surf. Sci. **38**, 433 (1973); Y. Bu and M. C. Lin, *ibid.* **298**, 94 (1993).
[19] M. C. Flowers, N. B. H. Jonathan, A. Morris, and S. Wright, Surf. Sci. **351**, 87 (1996).
[20] *CRC Handbook of Chemistry and Physics*, 81st ed., edited by D. R. Lide (CRC, Boca Raton, FL, 2001).
[21] J. P. Briand, Brigitte d'Etat, D. Schneider, M. Clark, and V. Decaux, Nucl. Instrum. Methods Phys. Res. B **87**, 138 (1994).